Turkish Journal of Electrical Engineering & Computer Sciences

http://journals.tubitak.gov.tr/elektrik/

Research Article

Turk J Elec Eng & Comp Sci
(2014) 22: 1540 – 1563

doi:10.3906/elk-1209-31

Contrast enhancement using linear image combinations algorithm (CEULICA) for enhancing brain magnetic resonance images

Burak YILMAZ*, **Yüksel ÖZBAY**
Department of Electrical & Electronics Engineering, Selçuk University, Konya, Turkey

Received: 07.09.2012 • **Accepted:** 21.02.2013 • **Published Online:** 07.11.2014 • **Printed:** 28.11.2014

Abstract: Brain magnetic resonance imaging (MRI) images support important information about brain diseases for physicians. Morphological alterations in brain tissues indicate the probable existence of a disease in many cases. Proper estimation of these tissues, measuring their sizes, and analyzing their image patterns are parts of the diagnosis process. Therefore, the interpretability and perceptibility level of the MRI image is valuable for physicians. In this paper, a new image contrast enhancement algorithm based on linear combinations is presented. The proposed algorithm is focused on improving the interpretability and perceptibility of the image information. An MRI image is presented to the algorithm, which generates a set of images from this MRI image. After this step, the algorithm uses the linear combination technique for combining the image set to generate a final image. Linear combination coefficients are generated using the artificial bee colony algorithm. The algorithm is evaluated by 4 different global image enhancement evaluation techniques: contrast improvement ratio (CIR), enhancement measurement error (EME), absolute mean brightness error (AMBE), and peak-signal-to-noise ratio (PSNR). During the evaluation process, 2 case studies are performed. The first case study is performed with 3 different image sets (T1, T2, and proton density) presented to the algorithm. These sets are obtained from the Brainweb simulated MRI database. The algorithm shows the best performance on the T1 image set with 5.844 CIR, 6.217 EME, 15.045 AMBE, and 22.150 dB PSNR scores as average values. The second case study is also performed with 3 different image sets (T1-fast low-angle shot sequence, T1-magnetization-prepared rapid acquired gradient-echoes (MP-RAGE), and T2) obtained from the The Multimedia Digital Archiving System public community database. The algorithm performs best with the T1-MP-RAGE modality images with 6.983 CIR, 17.326 EME, 3.514 AMBE, and 30.157 dB PSNR scores as average values. In addition, this algorithm can be used for classification tasks with proper linear combination coefficients, for instance, segmentation of the white matter regions in brain MRI images.

Key words: Image contrast enhancement, linear combination, artificial bee colony algorithm, image processing, MRI, multiple sclerosis

1. Introduction

Magnetic resonance imaging (MRI) technology has become a vital tool for clinical diagnosis in recent years. MRI technology is still advancing with new scanning and sequencing techniques. New innovations in this technology brought new opportunities and new improvements in diagnosing techniques. MRI technology supports the early diagnosis of many types of diseases, such as breast cancer, lung cancer, brain tumors, multiple sclerosis, and neurological irregularities. MRI technology has a noninvasive nature; hence, diagnosis techniques based on MRI are preferably applied to brain disease diagnosis. Various diseases appear as morphological alterations in

*Correspondence: burakyilmaz@selcuk.edu.tr

brain tissues. In the diagnosis process, proper estimation of these tissues, measuring their sizes, or analyzing their image patterns is crucial. Every diagnosis needs specific attention on specific regions of the brain image. For instance, when diagnosing multiple sclerosis, white matter (WM) regions are important and need to be examined more carefully. In some cases, the pattern of the cerebral cortex (CC) in the brain image needs to be focused on. Therefore, MRI images are segmented into specific regions for intense analyses. In some cases, unrelated regions in MRI images need to be removed, such as the skull, scalp, or fatty tissues. As a result, segmenting images as accurately as possible is beneficial.

There is a large variety of brain image segmentation algorithms reported in the literature. These algorithms can be categorized under methods based on intensity, atlas, region, probability, and hybrid methods [1–3]. These methods, especially the intensity- and region-based ones, have some difficulties due to inhomogeneity in intensity values, artifacts, and noise [4]. During the segmentation process, the effects of noise and intensity can cause overlaps on neighboring tissue classes. These overlaps induce erroneous segmentations [5]. Generally, to overcome this kind of problem, segmentation algorithms are preceded by a preprocessing step that includes image contrast enhancement algorithms. Image contrast enhancement is a common issue in image processing and computer vision. The main purpose of image enhancement in medical image processing is to adapt or improve the visual quality of images, for human eye sensitivity [6]. Moreover, improving the segmentation and classification success in semiautomated or automated image analysis systems is beneficial.

Contrast enhancement techniques can be categorized into 2 types, spatial and frequency domain [7]. Some of these techniques are defined as transformation functions, while others are defined as algorithms, including qualitative and quantitative analysis of the source image. Spatial domain techniques are the most popular techniques in image processing. Various spatial domain techniques are presented in the literature. Kabir et al. developed a technique based on a mixture of global and local transformation functions [7]. Kosheleva et al. modified the median filtering technique and developed the selective median filtering method [8]. Panetta et al. used edge-preserving contrast enhancement [9]. Chen et al. studied an automatic method for optimized image contrast enhancement [10]. Among these techniques, spatial bandpass filtering [11] and unsharp masking (USM) [9] can also be counted.

The methods mentioned above are successful and powerful, but brain MRI images have special properties, so not all techniques can reach the desired success rates. For instance, intensity levels of the skull affect the entire image histogram. Hence, extra attention is required for image contrast enhancement tasks in brain MRI. Another issue is the sequencing technique used to obtain a MRI image; for example, intensity values of specific tissues vary among the proton density (PD), T1, or T2 sequences. Thereby, a technique can be successful in the PD sequence but can also fail in the T2 sequence. To overcome these kinds of problems, specific contrast enhancement techniques have been developed in the literature. Khademi et al. developed an automated contrast enhancement technique that specifically works on fluid attenuated inversion recovery MRI [5]. Yang et al. used local bi-histogram equalization (HE) [12] and Vidaurrazaga et al. developed a technique based on the linear combination of wavelet coefficients [13].

This study aims to develop an adaptive technique for enhancing the contrast of the PD, T1, and T2 modality MRI images. The algorithm can be summarized in 3 main parts. First, the algorithm calculates index values and coefficients such as the median value of the histogram and darkening coefficients of the MRI image. Second, the algorithm generates 2 more images using these values. Next, some spatial filters are applied on the generated images. Finally, the enhanced image is obtained by the linear combination of the filtered images. Linear combination coefficients used by the algorithm are produced by the artificial bee colony

(ABC) algorithm developed by Karaboğa et al. [14,15]. The success of the algorithm is evaluated by 4 global contrast enhancement evaluation techniques: peak-signal-to-noise ratio (PSNR), enhancement measurement error (EME), absolute mean brightness error (AMBE), and contrast improvement ratio (CIR).

2. Methodology

The proposed method is an algorithm based on histogram adaptation methods. This algorithm is named the contrast enhancement using linear image combinations algorithm (CEULICA). It uses a grayscale image represented by integer values as an input and performs 19 steps for generating an output with the same data structure features. A flowchart of the algorithm is shown in Figure 1.

The original image presented to the algorithm is defined as g (x, y), and all images in the following formulations are defined as 2-dimensional matrices. The algorithm starts with applying an USM operation to the original image, as defined in Eqs. (1) and (2):

$$g(x, y) = f(x, y) - f_{smooth}(x, y), \tag{1}$$

$$f_{sharp}(x, y) = f(x, y) + kg(x, y), \tag{2}$$

while k is a scaling constant between 0.2–0.7 (in this study 0.5 is preferred).

After this step, the algorithm calculates the median value of the sharpened image and calculates the required constants as defined below:

$$\text{The histogram of the sharpened image is defined as } h(x), \tag{3}$$

$$m_h \text{ is the index of the median value of } h(x), \tag{4}$$

$$h_l(x) \text{ is the lower values than } m_h \text{ in } h(x), \tag{5}$$

$$h_u(x) \text{ is the higher values than } m_h \text{ in } h(x), \tag{6}$$

$$m_u \text{ is the index of the median value of } h_u(x), \tag{7}$$

$$m_l \text{ is the index of the median value of } h_l(x), \tag{8}$$

$$d(x, y) = f_{sharp}(x, y) - m_l, \tag{9}$$

$$l(x, y) = f_{sharp}(x, y) + m_u, \tag{10}$$

where $d(x, y)$ is the darkened version of $f_{sharp}(x, y)$ and $l(x, y)$ is the lightened version of $f_{sharp}(x, y)$. After generating these versions of the original image, the algorithm uses these images and generates a new set of images using linear combination techniques.

$$c_1(x, y) = \propto_1 f_{sharp}(x, y) + \propto_2 d(x, y) \tag{11}$$

$$c_2(x, y) = \propto_3 f_{sharp}(x, y) + \propto_4 l(x, y) \tag{12}$$

$$c_3(x, y) = \propto_5 c_1(x, y) + \propto_6 c_2(x, y) \tag{13}$$

$$c_4(x, y) = \propto_7 c_3(x, y) + \propto_8 f_{sharp}(x, y) \tag{14}$$

$$c_5(x, y) = c_4(x, y) - m_l \tag{15}$$

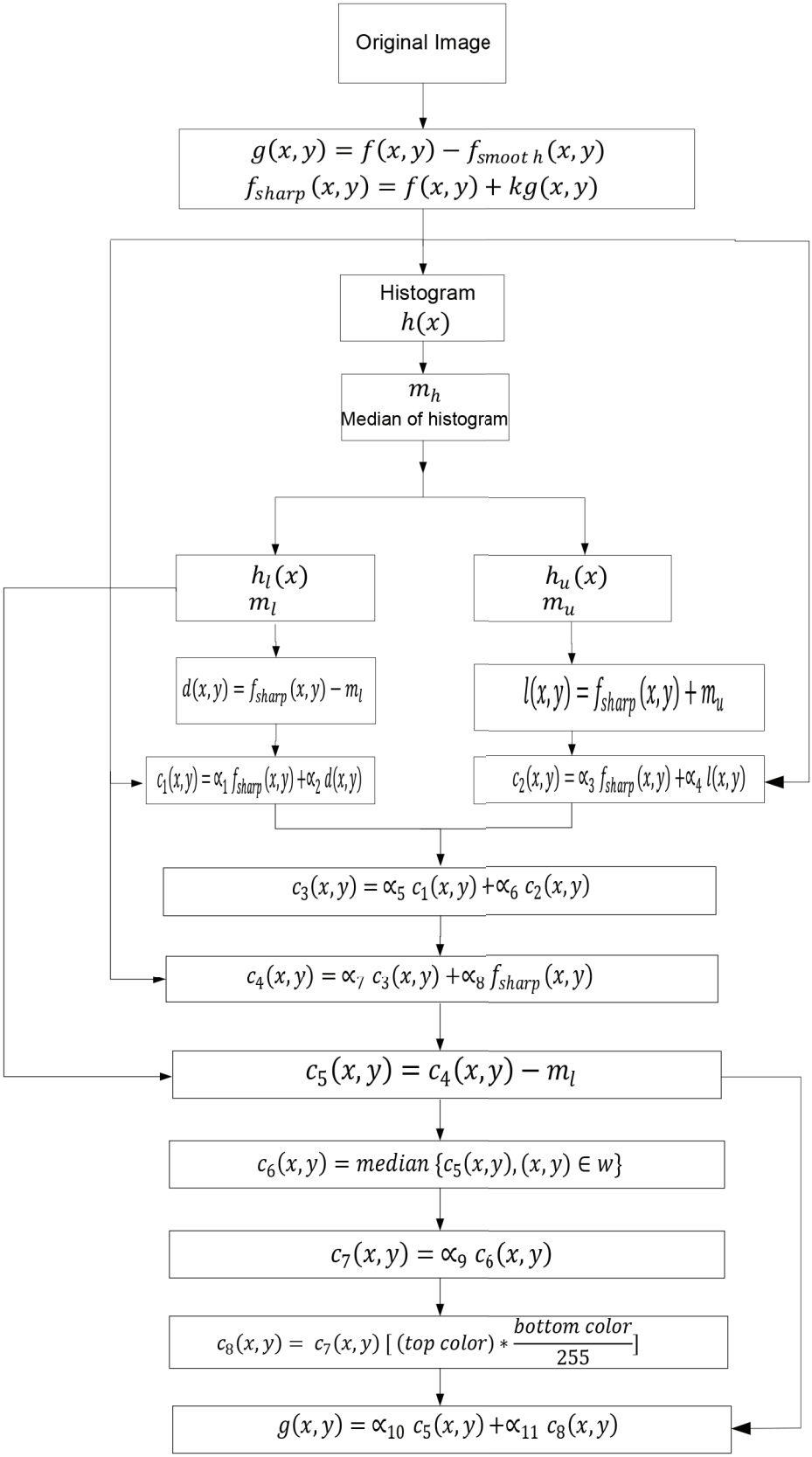

Figure 1. Flowchart of the algorithm.

$$c_6(x,y) = median\{c_5(x,y),\ (x,y) \in w \tag{16}$$

$$c_7(x,y) = \propto_9 c_6(x,y) \tag{17}$$

$$c_8(x,y) = c_7(x,y)\ [(top\,color) * \frac{bottom\,color}{255}] \tag{18}$$

$$g(x,y) = \propto_{10} c_5(x,y) + \propto_{11} c_8(x,y) \tag{19}$$

The final output image is represented as $g(x,y)$, and w is the neighborhood of (x,y). The coefficients $\{\propto_1 \propto_2, \ldots \propto_{11}\}$ are called as linear combination coefficients and they are produced by the ABC algorithm [15]. The ABC algorithm is used for finding the optimum values of these coefficients in this study. While finding the optimum values, the universal image quality index (UIQI) [16–18] value is used in the fitness function.

3. Generating the linear combination coefficient sets

The algorithm explained in the previous section requires 11 coefficients named linear combination coefficients $\{\propto_1 \propto_2, \ldots \propto_{11}\}$. These coefficients affect the quality of the final image, and so the values of these coefficients must be computed appropriately. In this study, the coefficient finding task is handled as a 'finding optimal solution in a search space' problem. The nature of the CEULICA requires an intense search of the coefficients, because each coefficient affects the others and sometimes their values appear to be close. Thus, a search algorithm based on neighborhood calculations is more suitable than other methods. The ABC algorithm is preferred because of its precision and search capacities.

The ABC algorithm simulates the food search task in a bee colony. While executing the algorithm, there are 3 types of bees. They are defined as employed bees, onlooker bees, and scout bees. Onlooker and scout bees are also defined as unemployed bees, all food source positions are discovered by scout bees, and the nectar of food sources is exploited by employed bees. Onlooker bees watch the employed bees to find the food sources [15].

The general algorithmic structure of the ABC optimization approach is given as follows [15]:

Initialization phase
REPEAT
    Employed bee phase
    Onlooker bee phase
    Scout bee phase
    Memorize the best solution achieved so far
UNTIL (cycle = maximum cycle number or a maximum central processing unit time)

The algorithm needs a fitness function for evaluating the success of the function with the values found after each search phase. The fitness function depends on the search task and it is generated specifically for the problem.

In this study, linear combination coefficients are imitated as food sources for employed bees. A fitness function for evaluating the adequacy of the coefficients is defined. The UIQI is used in the fitness function [16–18]. The UIQI function is a general image enhancement measuring function defined as:

The UIQI is defined as follows [16–18]:

$$x = \{x_i \,|i = 1,2,...,N\} \text{ and } y = \{y_i \,|i = 1,2,...,N\}, \tag{20}$$

$$Q = \frac{4\sigma_{xy}\overline{x}\overline{y}}{(\sigma_x^2 + \sigma_y^2)\left[(\overline{x})^2 + (\overline{y})^2\right]}, \tag{21}$$

$$\overline{x} = \frac{1}{N}\sum_{i=1}^{N} x_i, \overline{y} = \frac{1}{N}\sum_{i=1}^{N} y_i, \tag{22}$$

$$\sigma_x^2 = \frac{1}{N-1}\sum_{i=1}^{N} (x_i - \overline{x})^2, \sigma_y^2 = \frac{1}{N-1}\sum_{i=1}^{N} (y_i - \overline{y})^2, \tag{23}$$

$$\sigma_{xy}^2 = \frac{1}{N-1}\sum_{i=1}^{N} (x_i - \overline{x})(y_i - \overline{y}). \tag{24}$$

A source image and an enhanced image are presented to the UIQI function as parameters. Next, the UIQI function computes a value that is scaled between 0 and 1. In this scale, 0 means that the compared images are completely different and 1 means that the compared images are identical. If the value is closer to 1, this indicates that the enhancement is not sufficient. If the value is closer to 0, this indicates image lost information during the enhancement process.

During the experimental evaluations of the algorithm, values between 0.45 and 0.55 are accepted as optimum values. For obtaining the final value of the fitness function, the UIQI value is presented to a Gaussian function for computing the fitness of the optimum solution candidates. The Gaussian function is defined as follows:

$$f(x) = \frac{1}{\sigma\sqrt{2\pi}} e^{-(x-\mu)^2/(2\sigma^2)}. \tag{25}$$

The graphical representation of our fitness function is as in Figure 2.

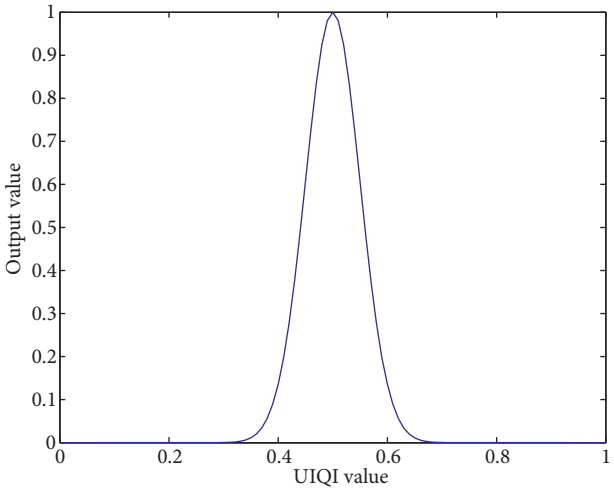

Figure 2. Graphical representation of the fitness function.

4. Brain image enhancements with the CEULICA

A magnetic resonance machine generates different types of images with different sequencing techniques. A MRI sequence comprises radio frequencies and gradient pulses combined in an order to acquire data from the tissues to form the image. There are many different sequencing techniques present in MRI technology. For example, the

T1, T2, PD, fast low-angle shot sequence (FLASH), and magnetization-prepared rapid acquired gradient-echoes (MP-RAGE)can be counted.

Images obtained by MRI machines have different features depending on the sequencing techniques, and so the image properties differ depending on the sequencing technique by which they are produced. For example, Figures 3a–3c show the 86th coronal slice of the simulated multiple sclerosis MRI from the Brainweb database [19–23], obtained with the T1, T2, and PD techniques, respectively. The histograms of the images are also shown in Figures 3d–3f, respectively, where it is seen that the same slices from the same tissues with different sequencing techniques have different properties.

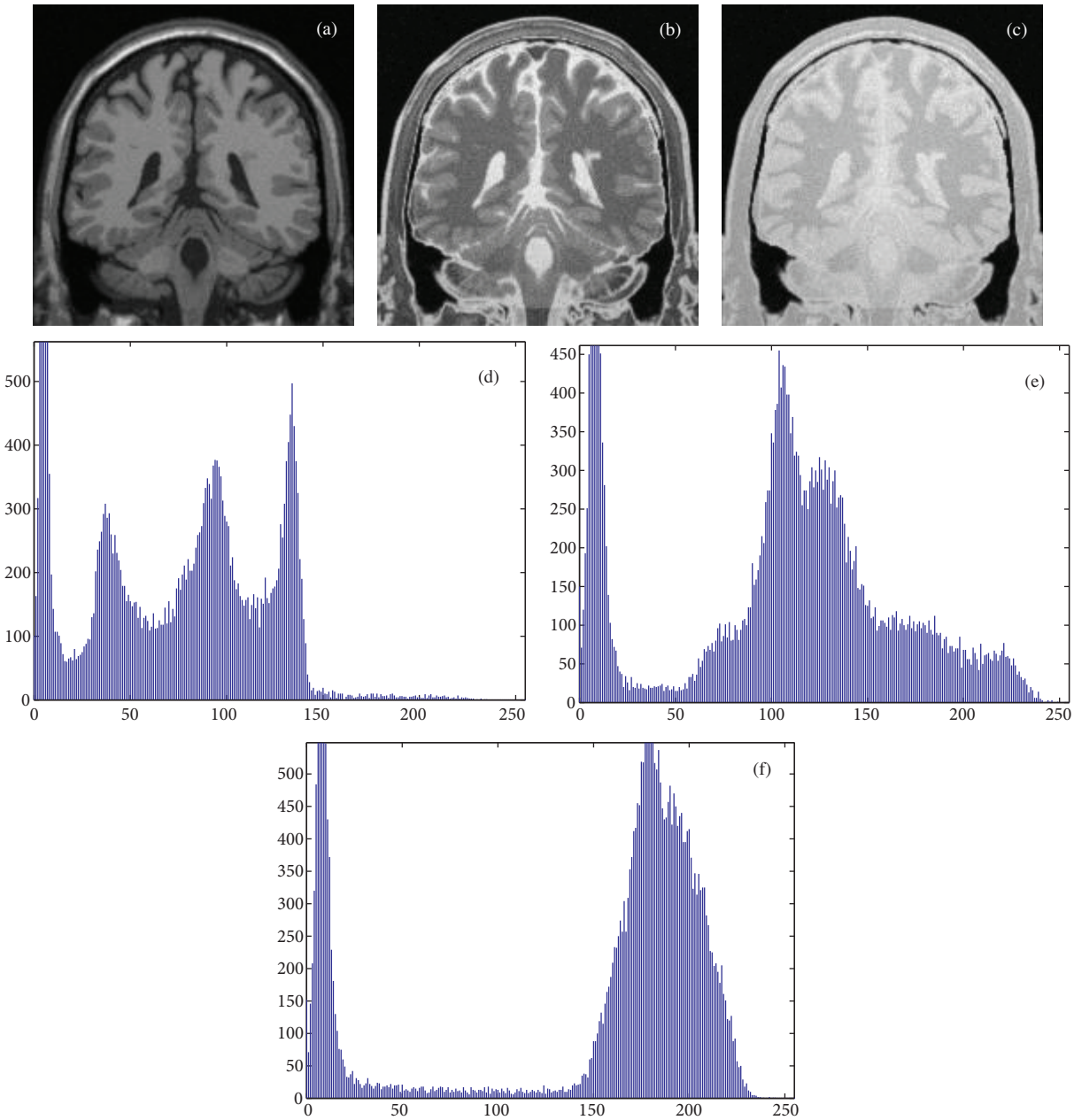

Figure 3. MRI images of the same slice: a) T1, b) T2, c) PD, d) histogram of T1, e) histogram of T2, and f) histogram of the PD.

In this study, the CEULICA needs different linear combination coefficients for different sequencing techniques. For this purpose, different coefficient sets for different sequences are generated by the ABC algorithm. After generating the coefficient sets, 2 case studies are performed with these sets. During the case studies, all of the image slices in the databases are processed using the CEULICA for evaluating the contrast enhancement performance of the algorithm. Next, the CEULICA generates a new enhanced image dataset. The entire process is performed on the T1, T2, and PD images from the Brainweb database and T1-MP-RAGE, T1-FLASH, and T2 modality images from the The Multimedia Digital Archiving System (MIDAS) [24] database.

The algorithm uses different coefficient sets for different MR image modalities. The coefficient sets are generated using the ABC algorithm is as follows:

Coefficient set for T1 (obtained from the Brainweb database), T1-MP-RAGE, and T1-FLASH (obtained from the MIDAS database):

$$\propto = \{-1.3364,\ 0.1359,\ -0.7102,\ 0.2326,\ 0.2647,\ 2,\ -0.21608,\ 0.9881,\ 0.54097,\ -0.2644,\ 0.1186\}.$$

Coefficient set for T2 (obtained from the Brainweb and MIDAS databases):

$$\propto = \{-0.1211,\ 0.5576,\ -0.9834,\ -2,\ 1.4984,\ 0.5089,\ -0.2491,\ 1.3623,\ 0.5396,\ -0.7227,\ -0.4607\}.$$

Coefficient set for the PD (obtained from the Brainweb database):

$$\propto = \{1.995, -1.093, -0.9758, 0.9074, 0.811, -0.4262, 1.0627, -0.0115, -1.0774, -1.7649, 1.649\}.$$

Every set is specific for only the modality that they are generated for. In this paper, we only generate sets for the T1, T2, and PD modalities, but more sets can be generated for different modalities. Coefficient sets generated for the T1 images are also used for the T1-FLASH and T1-MP-RAGE modalities.

5. Experimental results

The main purpose of this study is developing a new image enhancing technique for improving image contrast and helping segmentation tasks. The algorithm basically enhances the intensity level of tissues in brain MR images, while reducing the intensity level of the background. In addition, this algorithm can also be used for classification tasks with proper linear combination coefficients; for instance, segmentation of the WM regions in brain MRI images.

During the evaluation process, 2 case studies are performed. The first case study is performed on the Brainweb simulated brain image database [19]. The Brainweb database is a commonly used 3-dimensional database provided online from the McConnell Brain Imaging Center of the Montreal Neurological Institute of McGill University. The Brainweb database includes simulated MRI scans with 1-mm slice thickness, 3% noise, and 20% nonuniformity of only 1 patient. The dataset includes T1 weighted, T2 weighted, and PD magnetic resonance images subsets. Each subset contains 181 $\times$ 217 $\times$ 181 voxels. For evaluating the algorithm, 181 images (with 181 $\times$ 217 pixel resolution) are generated from every data subset. Each image among the 181 images is different from each other and so every image has different histogram properties. However, each image displays the general properties of the subset they belong to.

The second case study is performed on the MIDAS designed database of MR brain images of healthy volunteers [24]. Images are acquired on a 3T unit under standardized protocols. Images include T1 and T2

acquired at $1 \times 1 \times 1$ mm^3, magnetic resonance angiograpy acquired at $0.5 \times 0.5 \times 0.8$ mm^3, and diffusion tensor imaging using 6 directions and a voxel size of $2 \times 2 \times 2$ mm^3. In this study, the T1-FLASH, T1-MP-RAGE, and T2 sequences of the MIDAS database are used.

The algorithm's performance is evaluated by 4 global image enhancement evaluation methods: the EME, AMBE, PSNR [16–18], and CIR [5].

The evaluation methods can be formulized as follows:

EME [16–18] :

$$EME(\hat{f}) = EME_{\Phi}(\hat{f}) = \frac{1}{k^2}\sum_{m=1}^{k}\sum_{n=1}^{k} 20\log_2\frac{\max(\hat{f}\,[m,l])}{\min(\hat{f}\,[m,l])}. \tag{26}$$

AMBE [16–18] :

$$AMBE = |E(X) - E(Y)|\,. \tag{27}$$

CIR [5] :

$$CIR = \frac{\sum_{(x,y)\in\mathbf{R}} |c\,(x,y) - \tilde{c}(x,y)|^2}{\sum_{(x,y)\in\mathbf{R}} c\,(x,y)^2}. \tag{28}$$

The CIR is defined as a percentage and $c\,(x,y)$ and $\tilde{c}(x,y)$ are the local contrast values before and after enhancement, respectively. The local contrast value $C\,(x,y)$ is computed as follows:

$$C\,(x,y) = \frac{|p-a|}{p+a}, \tag{29}$$

where p and a are the mean values of the center region (3×3) of the selected pixel and surrounding region (7×7), respectively.

PSNR:

To compute the PSNR value, first the mean squared error must be calculated with the following equation:

$$MSE = \frac{\sum\limits_{M,N} [I_1\,(m,n) - I_2\,(m,n)]^2}{M \cdot N}, \tag{30}$$

where M and N are the number of rows and columns in the input images, respectively.

The PSNR value of an image is calculated by the following equation:

$$PSNR = 10\log_{10}\left(\frac{R^2}{MSE}\right), \tag{31}$$

where R is the maximum value that a pixel can get in the image. In this case, R is 255, which is the maximum value that can be defined with 8 bits for the Brainweb database and 4096 for the MIDAS database because of the 12-bit format of the database.

The values of these comparison criterions can be interpreted as follows:

Higher EME values indicate over enhancement and mean a local information loss. On the other hand, a very low EME value indicates that hidden information, such as lesions, is not significantly enhanced [17].

For the AMBE, very low or the highest values indicate poor performance in contrast enhancement [17].

The PSNR value compares the original image with the final image; the higher the PSNR value, the lower the distortions in the image. In this study, the PSNR value is used to determine the effects of the compared algorithms on noise in the MRI images.

The CIR defines the ratio of the enhancement between the original image and enhanced image; higher values mean higher enhancement qualities [5].

Results generated by the evaluation algorithms depend on the dataset, in which the algorithms are applied on; hence, the maximum, minimum, and optimum values are specific to the dataset.

Algorithms used in this comparison are the contrast limited adaptive HE (CLAHE), HE, and USM. Formulas of CLAHE, HE, and USM methods are defined as follows:

Matrix form of the USM:

$$f(\alpha) = \frac{1}{\alpha+1}\begin{bmatrix} -\alpha & \alpha-1 & -\alpha \\ \alpha-1 & \alpha+5 & \alpha-1 \\ -\alpha & \alpha-1 & -\alpha \end{bmatrix}. \tag{32}$$

CLAHE:

$$g = [g_{\max} - g_{\min}]\, p(f) + g_{\min}, \tag{33}$$

where $g_{\max}$ is the maximum pixel value, $g_{\min}$ is the minimum pixel value, g is the computed pixel value, and $p(f)$ is the cumulative probability distribution function.

HE:

$$p_n = \frac{\text{number of pixels with intensity}}{\text{total number of pixel}} \quad n = 0, 1, ..., L-1. \tag{34}$$

Histogram equalized image g will be defined by:

$$g_{i,j} = \text{ floor } ((L-1)\sum_{n=0}^{f_{i,j}} P_n. \tag{35}$$

5.1. Case study 1

In case study 1, the performance of the CEULICA is evaluated with the Brainweb database. The slices in the Brainweb datasets start from the front of the head, and a higher slice number means an interior brain slice from the front to the end of the head.

Tables 1–3 represent the performance evaluation scores of the enhancement algorithms (CLAHE, HE, USM, and CEULICA) with different sequencing techniques (T1, T2, and PD). The rows show the performance scores of the enhancement algorithms and the columns show the different evaluation techniques (CIR, EME, AMBE, and PSNR). The entire Brainweb database (181 slices) is processed by the enhancement algorithms. Only a few slice numbers are shown in the tables for shortening the table size, but average values placed at the end of the tables show the average scores of the evaluation techniques applied on all of the enhancement algorithms.

Table 1 presents the enhancement comparisons of the Brainweb database with T1 modality, 1-mm slice thickness, 3% noise, and 20% nonuniformity. The T1 data includes 181 images with 181 $\times$ 217 pixel resolution.

As seen in Table 1, the CEULICA is scored by 5.844 CIR, 6.217 EME, 15.045 AMBE, and 22.15 dB PSNR as average values.

Table 1. Quantitative performance measures compared to 4 different enhancing algorithms for the T1 modality.

Slice	CIR				EME				AMBE				PSNR (dB)			
number	*CLAHE*	*HE*	*USM*	***CEULICA***	*CLAHE*	*HE*	*USM*	***CEULICA***	*CLAHE*	*HE*	*USM*	***CEULICA***	*CLAHE*	*HE*	*USM*	***CEULICA***
1	0.016	1.431	0.006	**1**	9.329	22.546	18.907	**0**	12.929	122.56	0.003	**4.938**	25.583	5.131	50.092	**33.939**
2	0.015	1.498	0.007	**1**	9.366	23.1	18.77	**0**	12.9	122	0.003	**4.97**	25.62	5.144	50.08	**33.89**
3	0.016	1.497	0.006	**1**	9.245	22.517	18.736	**0**	12.934	122.78	0.003	**4.961**	25.584	5.114	50.136	**33.9**
—																
20	0.05	0.954	0.004	**9.486**	9.278	15.47	15.66	**2.392**	23.16	106	0.003	**6.418**	18.02	6.655	48.5	**24.56**
21	0.052	0.872	0.004	**8.839**	9.401	15.26	15.869	**2.887**	23.759	105.45	0.003	**5.679**	17.835	6.724	48.374	**24.35**
22	0.058	0.897	0.004	**8.963**	9.349	14.648	15.636	**2.664**	24.098	105.05	0.002	**6.694**	17.683	6.782	48.329	**24.477**
—																
160	0.116	0.453	0.002	**4.827**	10.84	7.663	13.1	**6.868**	29.33	67.02	0.004	**16.03**	16.6	11	45.43	**21.67**
161	0.117	0.458	0.002	**4.578**	10.68	7.764	12.96	**6.921**	29.18	67.92	0.004	**14.59**	16.63	10.88	45.51	**22.27**
162	0.116	0.502	0.002	**4.45**	10.56	7.929	13.16	**6.729**	28.93	68.58	0.004	**14.14**	16.7	10.79	45.66	**22.4**
—																
180	0.095	0.615	0.002	**4.717**	11.06	12.37	15.18	**6.384**	30.48	83.65	0.003	**12.91**	16.01	8.942	46.2	**23.01**
181	0.094	0.73	0.002	**5.244**	10.55	9.762	14.63	**6.223**	29.9	84.53	0.003	**12.49**	16.09	8.82	46.34	**23.12**
Average	0.117	0.493	0.002	**5.844**	10.19	9.567	12.35	**6.217**	31.37	72.08	0.004	**15.05**	16.16	10.41	46.3	**22.15**

Table 2. Quantitative performance measures compared to 4 different enhancing algorithms for the T2 modality.

Slice	CIR				EME				AMBE				PSNR (dB)			
number	*CLAHE*	*HE*	*USM*	***CEULICA***	*CLAHE*	*HE*	*USM*	***CEULICA***	*CLAHE*	*HE*	*USM*	***CEULICA***	*CLAHE*	*HE*	*USM*	***CEULICA***
1	0.016	1.431	0.006	**1.000**	9.329	22.546	18.907	0.000	12.929	122.56	0.003	4.938	25.583	5.131	50.092	33.939
2	0.015	1.498	0.007	**1.000**	9.366	23.097	18.772	0.000	12.896	122.04	0.003	4.970	25.615	5.144	50.080	33.887
3	0.016	1.497	0.006	**1.000**	9.245	22.517	18.736	0.000	12.934	122.77	0.003	4.961	25.584	5.114	50.136	33.900
—																
20	0.050	0.954	0.004	**8.665**	9.278	15.468	15.661	4.631	23.163	106.04	0.003	5.756	18.019	6.655	48.496	15.256
21	0.052	0.872	0.004	**8.325**	9.401	15.260	15.869	4.939	23.759	105.45	0.003	5.290	17.835	6.724	48.374	15.077
22	0.058	0.897	0.004	**8.186**	9.349	14.648	15.636	5.203	24.098	105.048	0.002	5.609	17.683	6.782	48.329	14.883
—																
160	0.116	0.453	0.002	**4.365**	10.835	7.663	13.102	10.088	29.334	67.023	0.004	26.809	16.600	10.998	45.427	11.292
161	0.117	0.458	0.002	**4.428**	10.682	7.764	12.962	10.004	29.178	67.923	0.004	26.325	16.627	10.878	45.513	11.322
162	0.116	0.502	0.002	**4.541**	10.561	7.929	13.160	9.915	28.927	68.577	0.004	25.721	16.696	10.786	45.658	11.333
—																
180	0.095	0.615	0.002	**3.826**	11.062	12.372	15.180	9.000	30.475	83.646	0.003	16.209	16.010	8.942	46.201	12.699
181	0.094	0.730	0.002	**4.076**	10.553	9.762	14.627	8.739	29.900	84.526	0.003	15.026	16.094	8.820	46.336	12.807
Average	0.117	0.493	0.002	**4.736**	10.188	9.567	12.353	**9.251**	31.372	72.083	0.004	**17.652**	16.161	10.414	46.303	**12.680**

Table 3. Quantitative performance measures compared to 4 different enhancing algorithms for the PD modality.

Slice	CIR				EME				AMBE				PSNR (dB)			
number	*CLAHE*	*HE*	*USM*	***CEULICA***	*CLAHE*	*HE*	*USM*	***CEULICA***	*CLAHE*	*HE*	*USM*	***CEULICA***	*CLAHE*	*HE*	*USM*	***CEULICA***
1	0.016	1.431	0.006	**1.000**	9.329	22.546	18.907	**0.000**	12.929	122.52	0.003	**4.938**	25.583	5.131	50.092	**33.939**
2	0.015	1.498	0.007	**1.000**	9.366	23.097	18.772	**0.000**	12.896	122.00	0.003	**4.970**	25.615	5.144	50.080	**33.887**
3	0.016	1.497	0.006	**1.000**	9.245	22.517	18.736	**0.000**	12.934	122.75	0.003	**4.961**	25.584	5.114	50.136	**33.900**
—																
20	0.050	0.954	0.004	**6.705**	9.278	15.468	15.661	**2.458**	23.163	106.040	0.003	**6.821**	18.019	6.655	48.496	**20.096**
21	0.052	0.872	0.004	**6.538**	9.401	15.260	15.869	**2.638**	23.759	105.454	0.003	**8.028**	17.835	6.724	48.374	**20.117**
22	0.058	0.897	0.004	**6.441**	9.349	14.648	15.636	**2.885**	24.098	105.048	0.002	**6.127**	17.683	6.782	48.329	**19.689**
—																
160	0.116	0.453	0.002	**3.280**	10.835	7.663	13.102	**5.493**	29.334	67.023	0.004	**19.513**	16.600	10.998	45.427	**15.694**
161	0.117	0.458	0.002	**3.420**	10.682	7.764	12.962	**5.372**	29.178	67.923	0.004	**20.222**	16.627	10.878	45.513	**15.621**
162	0.116	0.502	0.002	**3.283**	10.561	7.929	13.160	**5.437**	28.927	68.577	0.004	**19.863**	16.696	10.786	45.658	**15.659**
—																
180	0.095	0.615	0.002	**3.092**	11.062	12.372	15.180	**4.775**	30.475	83.646	0.003	**12.340**	16.010	8.942	46.201	**17.399**
181	0.094	0.730	0.002	**3.338**	10.553	9.762	14.627	**4.683**	29.900	84.526	0.003	**11.747**	16.094	8.820	46.336	**17.531**
Average	0.117	0.493	0.002	**3.594**	10.188	9.567	12.353	**4.871**	31.372	72.083	0.004	**16.209**	16.161	10.414	46.303	**17.211**

Table 2 presents enhancement comparisons of the Brainweb database with T2 modality, 1-mm slice thickness, 3% noise, and 20% nonuniformity. These data include 181 images with 181 × 217 pixel resolution.

As seen in Table 2, the CEULICA is scored by 4.736 CIR, 9.251 EME, 17.652 AMBE, and 12.68 dB PSNR as average values.

Table 3 presents enhancement comparisons of the Brainweb database with PD modality, 1-mm slice thickness, 3% noise, and 20% nonuniformity. These data include 181 images with 181 × 217 pixel resolution.

As seen in Table 3, the CEULICA is scored by 3.594 CIR, 4.871 EME, 16.209 AMBE, and 17.211 dB PSNR as average values.

In Figure 4, the T1, T2, and PD versions of the 86th slice of the Brainweb database are shown in Figures 4a–4c, respectively, and the histograms of the enhanced images in Figures 4d–4f are shown in the same order.

5.2. Case study 2

In case study 2, the performance of the CEULICA was evaluated with the MIDAS database. For evaluation, 186 MRI scans are selected from the MIDAS database [24]. Table 4 represents information about every scan obtained from the 97 volunteers. These scans are in the T1-FLASH, T1-MP-RAGE, and T2 modalities. Some volunteers do not have some modality scans; thus 186 scans are investigated in this study. Every scan has a different numbers of slices, and the total slice number of these 186 scans is 27,504. The images obtained from the MIDAS database are in MetaImage format; thus images are represented as 12-bit integer values [24].

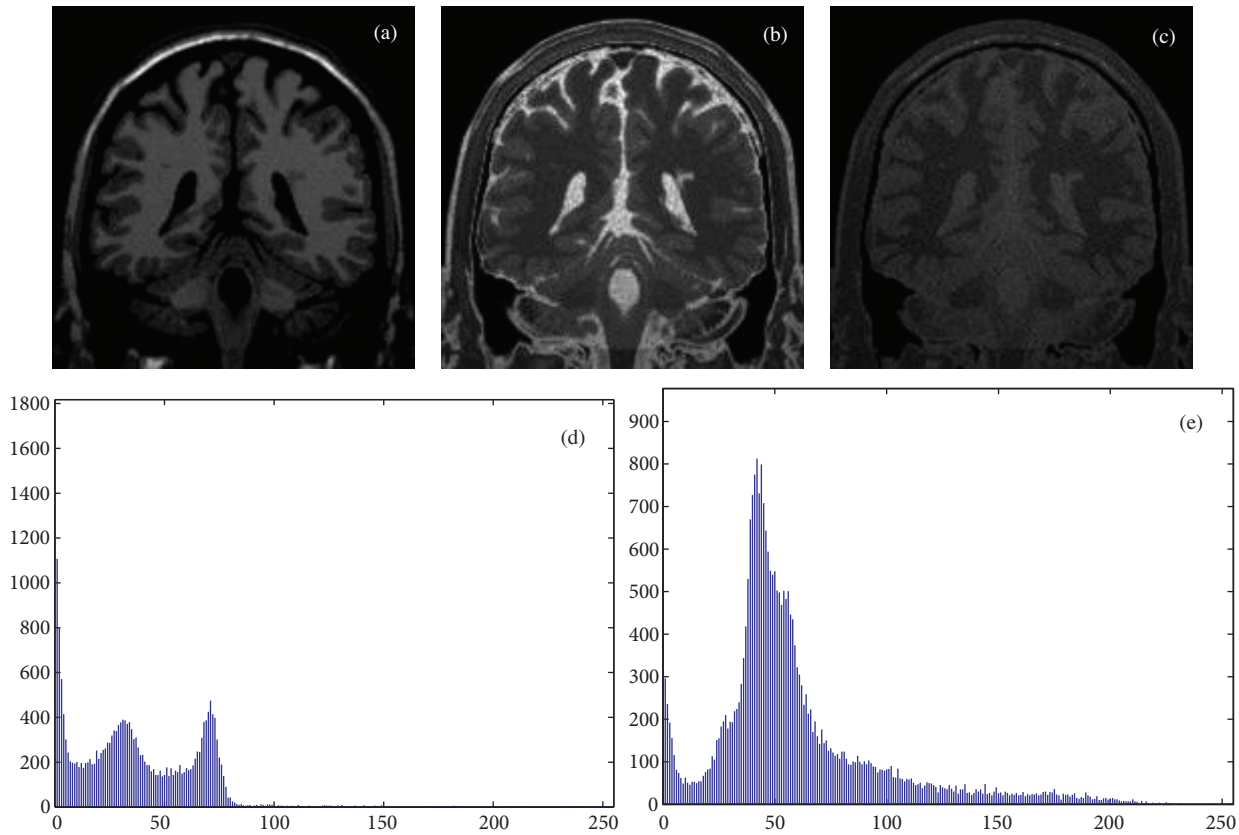

Figure 4. MRI images of the same slice after enhancing with the CEULICA: a) T1, b) T2, c) PD, d) histogram of T1, e) histogram of T2,

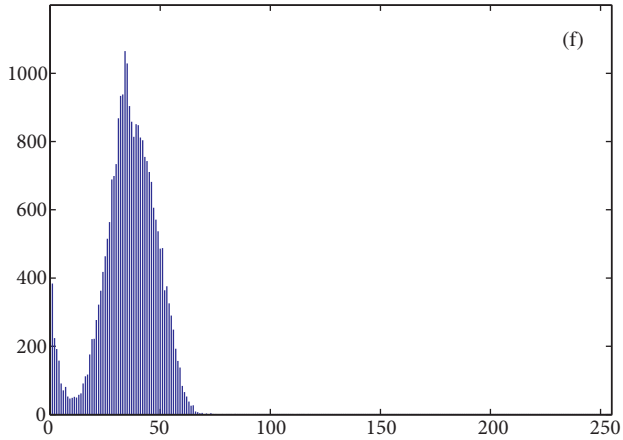

Figure 4. MRI images of the same slice after enhancing with the CEULICA: f) histogram of the PD.

Tables 5–7 present our algorithm's performance evaluation values with different sequencing techniques and specific combination coefficients for the modalities, where rows show the performance scores of the algorithms and columns show different evaluation algorithm scores.

The entire MIDAS database (186 files, 27,504 slices) is processed by the algorithms, but only a few results are shown in the tables for shortening the table size. Average values placed at the end of the tables show the average scores obtained with the entire evaluation process.

As seen in Table 5, the CEULICA is scored by 6.983 CIR, 17.326 EME, 3.514 AMBE, and 30.157 dB PSNR as average values.

As seen in Table 6, the CEULICA is scored by 10.191 CIR, 12.82 EME, 2.884 AMBE and 30.948 dB PSNR as average values.

As seen in Table 7, the CEULICA is scored by 2.705 CIR, 73.111 EME, 2.073 AMBE, and 20.24 dB PSNR as average values.

The T1-MP-RAGE, T1-FLASH, and T2 versions of the 100th slice of the 28th volunteer in the MIDAS database are shown in Figure 5.

The results shown in Tables 1–7 (case studies 1 and 2) present the enhancement performance of the CEULICA, where it can be seen that the evaluation scores of the CEULICA are neither the highest nor the lowest values, which is a desired result showing the success of the algorithm. The CEULICA's performance with the PD images is not sufficient among the other subsets. In case study 1, the algorithm achieves a lower PSNR score than the USM algorithm in all of the evaluations, which means that the USM algorithm suppresses the noise more successfully than the CEULICA with the Brainweb database. In contrast, in case study 2, the algorithm achieved a higher PSNR score than the other enhancement algorithm, which means that the CEULICA suppresses the noise more successfully with the MIDAS database. PSNR scores show that the CEULICA is more successful with the MIDAS database than the Brainweb database.

Usage of the CEULICA for classification:

There is another yield of the algorithm. The CEULICA can also be used for classification tasks. For this purpose, the only need is to find the right coefficient sets for classifications. With proper coefficients, the algorithm can perform many different classifications. The following sets and images present this ability of the algorithm. The 86th, 136th, and 181st images of the Brainweb database are used in this brief representation. Thus, 3 coefficient sets are generated for the T1, T2, and PD modality images.

Table 4. Information about the MIDAS database as slice number and pixels.

Volunteer	T1-FLASH		T1-MP-RAGE		T2	
number	Slice number	Image size (pixels)	Slice number	Image size (pixels)	Slice number	Image size (pixels)
3	176	176 × 256	NA	NA	128	192 × 256
4	176	176 × 256	NA	NA	128	192 × 256
20	NA	NA	NA	NA	128	192 × 256
21	176	176 × 256	NA	NA	NA	NA
27	NA	NA	NA	NA	128	192 × 256
28	176	176 × 256	128	208 × 256	128	192 × 256
29	176	176 × 256	128	208 × 256	NA	NA
30	176	176 × 256	NA	NA	128	192 × 256
31	NA	NA	128	208 × 256	128	192 × 256
32	176	176 × 256	NA	NA	128	192 × 256
34	176	176 × 256	128	208 × 256	NA	NA
37	176	176 × 256	128	208 × 256	NA	NA
41	176	176 × 256	128	208 × 256	128	192 × 256
42	NA	NA	128	208 × 256	128	192 × 256
43	176	176 × 256	128	208 × 256	NA	NA
46	NA	NA	128	208 × 256	NA	NA
47	176	176 × 256	128	208 × 256	NA	NA
49	176	176 × 256	128	208 × 256	128	192 × 256
50	176	176 × 256	128	208 × 256	NA	NA
53	176	176 × 256	NA	NA	128	192 × 256
54	176	176 × 256	128	208 × 256	NA	NA
56	176	176 × 256	NA	NA	NA	NA
59	176	176 × 256	NA	NA	NA	NA
60	NA	NA	128	208 × 256	128	192 × 256
62	176	176 × 256	NA	NA	128	192 × 256
66	NA	NA	128	208 × 256	128	192 × 256
69	NA	NA	128	208 × 256	128	192 × 256
72	NA	NA	NA	NA	128	192 × 256
73	176	176 × 256	NA	NA	128	192 × 256
74	176	176 × 256	160	208 × 256	128	192 × 256
75	NA	NA	160	208 × 256	NA	NA
76	NA	NA	160	208 × 256	128	192 × 256
80	160	176 × 256	160	208 × 256	128	192 × 256
82	NA	NA	160	208 × 256	128	192 × 256
83	NA	NA	160	208 × 256	NA	NA
86	NA	NA	NA	NA	128	192 × 256
88	160	176 × 256	NA	NA	NA	NA
89	160	176 × 256	160	208 × 256	128	192 × 256
90	160	176 × 256	160	208 × 256	NA	NA
91	160	176 × 256	NA	NA	NA	NA
96	NA	NA	NA	NA	160	392 × 512
97	NA	NA	160	208 × 256	NA	NA
100	NA	NA	160	208 × 256	NA	NA
101	NA	NA	160	208 × 256	160	392 × 512
102	NA	NA	NA	NA	NA	NA
103	NA	NA	160	208 × 256	NA	NA
106	NA	NA	160	208 × 256	160	392 × 512
107	NA	NA	160	208 × 256	NA	NA

Table 5. Quantitative performance measures compared to 4 different enhancing algorithms for the MP-RAGE modality.

Slice number	CIR				EME				AMBE				PSNR (dB)			
	CLAHE	*HE*	*USM*	***CEULICA***	*CLAHE*	*HE*	*USM*	***CEULICA***	*CLAHE*	*HE*	*USM*	***CEULICA***	*CLAHE*	*HE*	*USM*	***CEULICA***
031-T1-MP-RAGE	0.071	0.495	0.144	0.442	45.733	36.554	3.828	18.182	19.717	88.743	3.972	0.832	20.044	8.432	21.594	37.605
—																
081-T1-MP-RAGE	0.067	0.467	0.150	2.905	44.479	37.920	4.488	15.847	23.304	89.977	3.400	0.943	18.488	8.353	21.948	35.860
083-T1-MP-RAGE	0.087	0.489	0.153	15.667	44.020	38.079	4.181	12.761	24.973	99.084	2.908	1.161	17.710	7.405	23.700	34.904
—																
100-T1-MP-RAGE	0.120	0.460	0.164	15.050	45.763	40.865	4.510	13.474	30.958	90.018	2.596	11.862	16.003	8.337	22.741	11.656
101-T1-MP-RAGE	0.134	0.511	0.171	8.982	46.370	46.131	3.505	10.270	23.716	93.615	2.898	6.758	17.946	7.873	23.167	12.917
103-T1-MP-RAGEe	0.121	0.484	0.195	3.874	45.594	47.723	4.059	11.217	26.148	96.165	2.900	7.281	17.277	7.631	23.515	12.401
106-T1-MP-RAGE	0.103	0.458	0.171	17.795	46.620	38.881	4.162	14.470	30.165	94.234	2.689	12.094	16.238	7.893	23.494	11.635
Average	0.115	0.430	0.171	**6.983**	46.359	39.848	4.708	**17.326**	23.858	90.459	3.509	**3.514**	18.717	8.281	22.254	**30.157**

Table 6. Quantitative performance measures compared to 4 different enhancing algorithms for the FLASH modality.

Slice number	CIR				EME				AMBE				PSNR (dB)			
	CLAHE	*HE*	*USM*	***CEULICA***	*CLAHE*	*HE*	*USM*	***CEULICA***	*CLAHE*	*HE*	*USM*	***CEULICA***	*CLAHE*	*HE*	*USM*	***CEULICA***
023-T1-Flash	0.101	0.499	0.178	9.878	41.481	32.270	4.362	**10.572**	25.069	101.527	2.680	**1.788**	17.444	7.234	24.061	**34.482**
—																
085-T1-Flash	0.132	0.518	0.186	3.771	41.638	38.232	5.036	**9.245**	27.878	99.444	2.647	**5.737**	16.803	7.385	23.416	**17.552**
087-T1-Flash	0.123	0.512	0.188	3.653	43.667	38.090	4.441	**11.431**	29.091	101.025	2.658	**4.572**	16.475	7.190	23.402	**18.044**
088-T1-Flash	0.116	0.511	0.172	7.467	42.426	30.353	5.401	**11.455**	29.926	95.664	2.797	**6.699**	16.236	7.758	22.621	**18.627**
091-T1-Flash	0.104	0.405	0.174	0.146	45.213	37.731	6.329	**15.715**	35.448	92.830	3.301	**9.588**	15.056	7.996	21.731	**15.712**
093-T1-Flash	0.115	0.454	0.164	0.387	43.503	37.879	5.921	**13.329**	33.778	94.053	3.006	**8.856**	15.405	7.875	22.184	**16.049**
094-T1-Flash	0.112	0.428	0.171	0.332	44.160	40.546	5.327	**12.866**	34.732	94.561	2.992	**7.862**	15.332	7.787	22.234	**15.780**
Average	0.112	0.483	0.177	**10.191**	43.534	34.304	5.068	**12.820**	26.291	97.541	2.991	**2.884**	17.660	7.611	22.966	**30.948**

Table 7. Quantitative performance measures compared to 4 different enhancing algorithms for the T2 modality.

Slice	CIR				EME				AMBE				PSNR (dB)			
number	*CLAHE*	*HE*	*USM*	***CEULICA***	*CLAHE*	*HE*	*USM*	***CEULICA***	*CLAHE*	*HE*	*USM*	***CEULICA***	*CLAHE*	*HE*	*USM*	***CEULICA***
014-T2	0.859	0.361	0.244	**1.739**	46.346	87.371	2.985	**59.764**	12.338	8.973	21.705	**5.115**	8.559	26.473	2.655	**21.358**
—																
061-T2	0.978	0.439	0.217	**2.452**	54.523	97.444	2.415	**74.048**	11.355	7.414	21.234	**-1.232**	10.535	25.447	1.270	**20.911**
062-T2	0.860	0.421	0.185	**2.162**	82.956	88.158	2.652	**66.935**	11.013	9.255	22.486	**3.271**	8.838	30.913	1.735	**14.056**
—																
096-T2	0.855	0.589	0.046	**0.592**	5.034	92.638	0.837	**3.197**	32.043	8.006	28.565	**17.459**	58.337	34.956	8.105	**19.262**
099-T2	0.893	0.505	0.048	**0.813**	8.176	90.825	0.749	**5.305**	26.780	8.196	28.387	**17.776**	43.603	18.810	9.562	**21.520**
101-T2	0.856	0.575	0.049	**0.579**	5.110	97.350	0.812	**4.607**	31.583	7.545	29.246	**17.953**	58.354	36.503	7.606	**18.531**
106-T2	0.907	0.537	0.065	**0.772**	19.712	95.936	0.817	**14.693**	13.886	7.757	29.690	**15.509**	39.819	23.378	9.209	**21.669**
Average	0.937	0.425	0.205	**2.705**	64.716	94.864	2.595	**73.111**	12.049	7.947	22.231	**2.073**	12.683	30.776	2.777	**20.240**

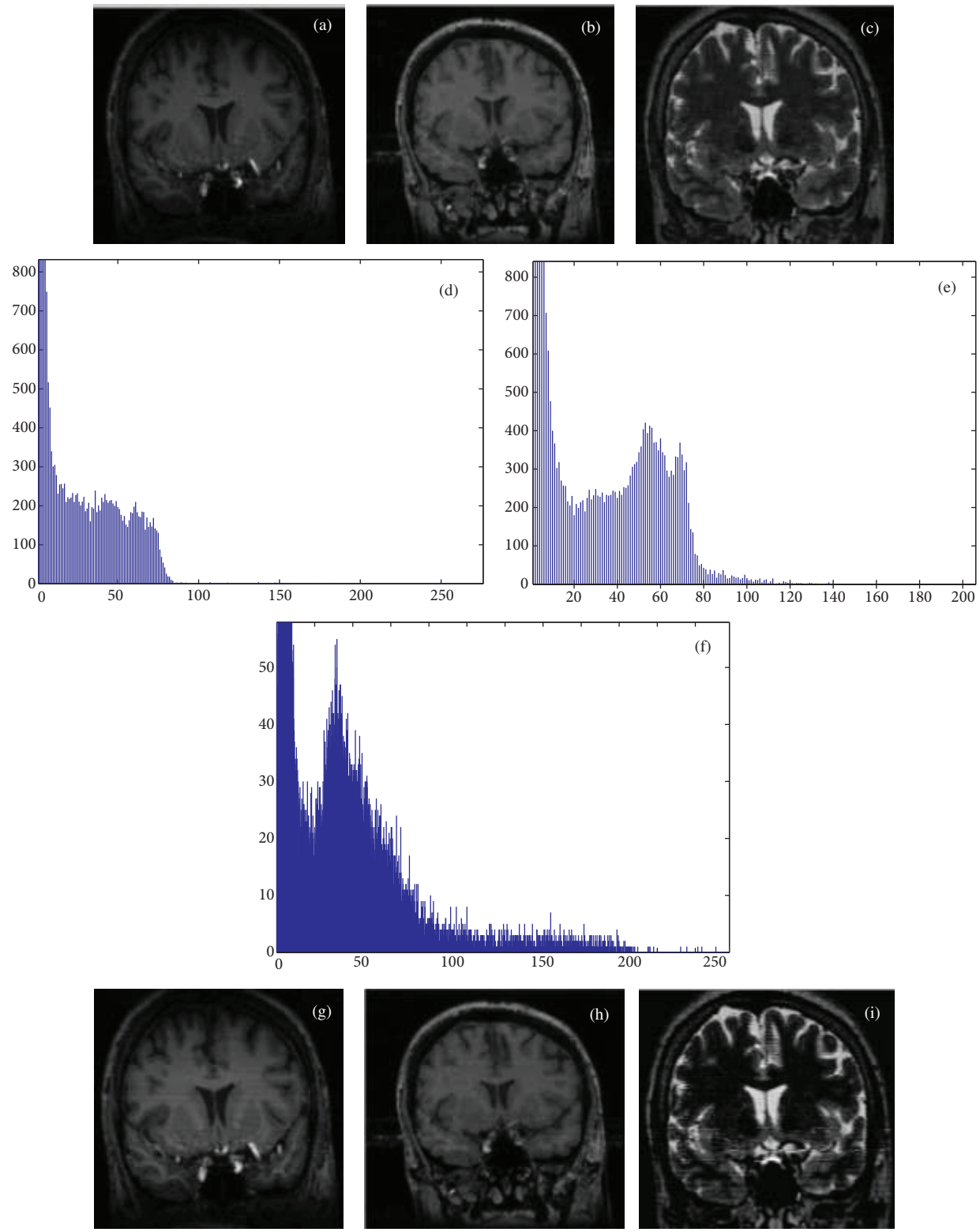

Figure 5. MRI images before and after enhancement with the CEULICA: a) T1-MP-RAGE, b) T1-FLASH, c) T2, d) histogram of T1-MP-RAGE, e) histogram of T1-FLASH, f) histogram of T2, g) enhanced T1-MP-RAGE, h) enhanced T1-FLASH and i) enhanced T2.

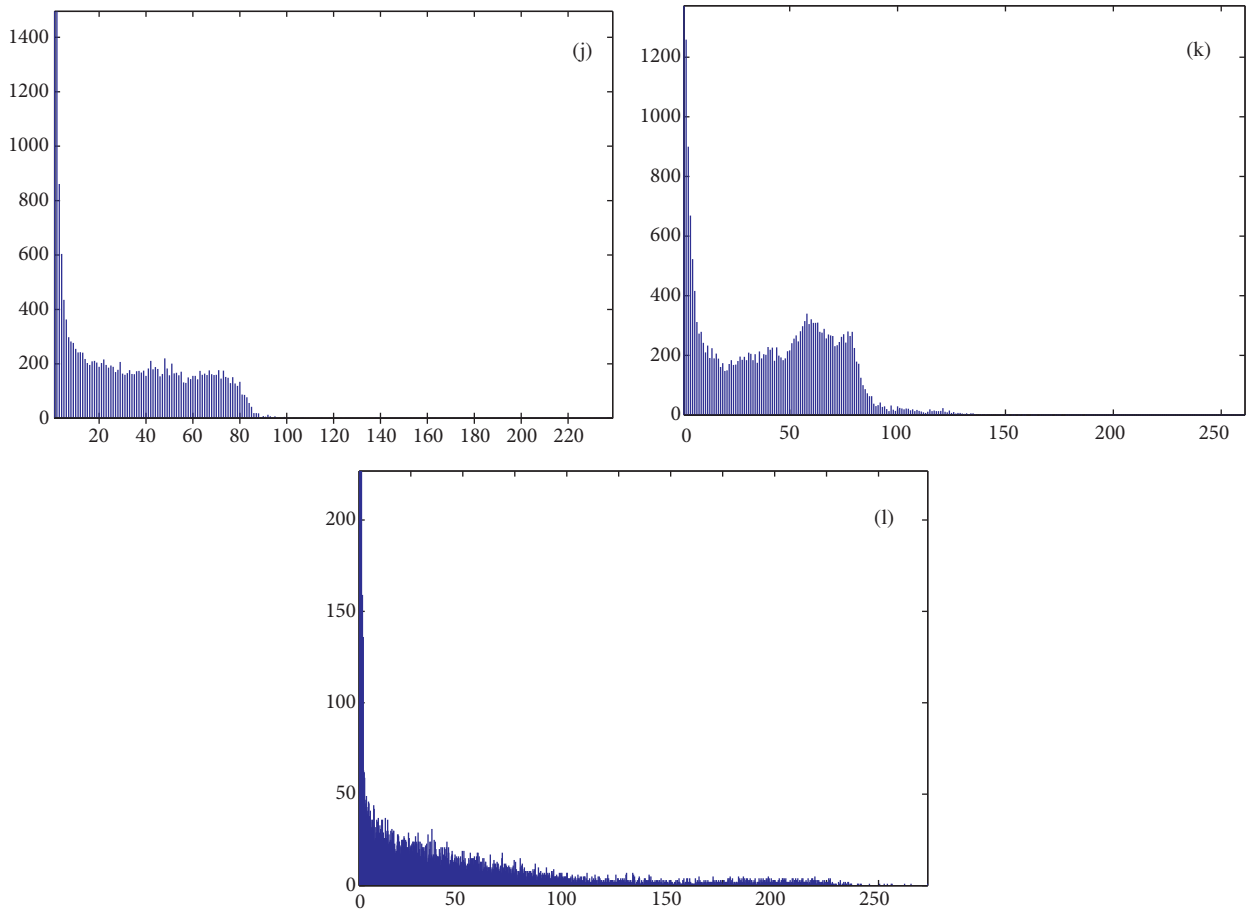

Figure 5. MRI images before and after enhancement with the CEULICA: j) histogram of the enhanced T1-MP-RAGE, k) histogram of the enhanced T1-FLASH, and l) histogram of the enhanced T2.

Coefficient set for the T1 modality:

$\propto = \{1.426, -1.934, 0.24375, -1.358, 0.504, 2, 0.329, 0.421, 0.484, -1.097, -0.792\}$.

With this set, the algorithm enhances the WM region in the brain and the results are shown in Figures 6a–6c.

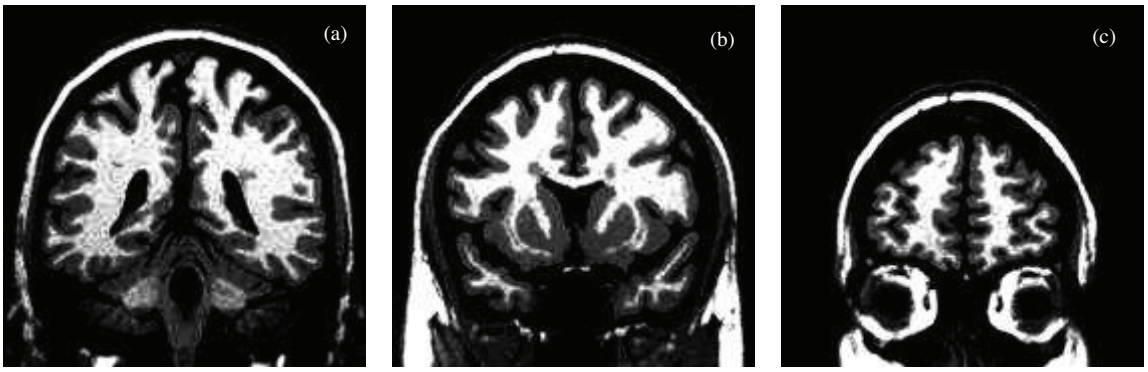

Figure 6. a) 86th image of the set, b) 136th image of the set, and c) 181st image of the set.

Coefficient set for the T2 modality:

$\propto$= {3.622, 1.893, 2.069, 0.4756, –1.684, –4, 2.865, 0.387, 3.844, –3.844, –0.543}.

With this set, the algorithm enhances the CC region in the brain and the results are shown in Figures 7a–7c.

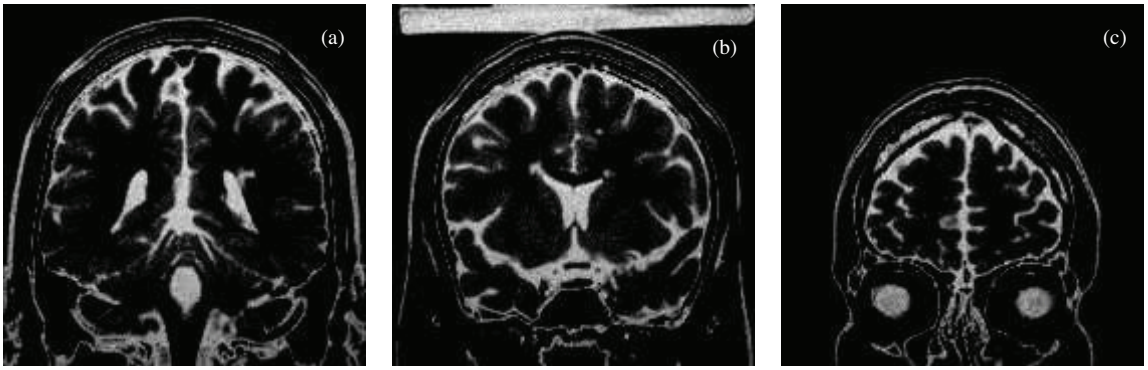

Figure 7. a) 86th image of the set, b) 136th image of the set, and c) 181st image of the set.

Coefficient set for the PD modality:

$\propto$= {3.622, 1.893, 2.069, 0.475, –1.684, –4, 2.861, 0.387, 3.844, –3.844, –0.543}.

With this set, the algorithm enhances the whole brain and skull regions in the brain and the results are shown in Figures 8a–8c.

Figure 8. a) 86th image of the set, b) 136th image of the set, and c) 181st image of the set.

6. Conclusions

In this paper, a new image contrast enhancement algorithm for brain MRI images is presented. The Brainweb and MIDAS databases are used for evaluating the algorithm. In this study, the performance of the proposed algorithm is evaluated on both 8-bit and 12-bit grayscale images. For the 8-bit image set, the Brainweb database is used, which comprises T1, T2, and PD modality image scans of a multiple sclerosis simulated brain scan with 1-mm slice thickness, 3% noise, and 20% nonuniformity. This database includes 181 images with 181 $\times$ 217 pixel resolution.

For the 12-bit image set, the MIDAS database used. The MIDAS database consists of MR brain images of healthy volunteers. Images are acquired on a 3T unit under standardized protocols. Images include T1 and T2 acquired at $1 \times 1 \times 1$ mm^3. In this study, the T1-FLASH, T1-MP-RAGE, and T2 sequences of the MIDAS database are used.

The algorithm operates with a coefficient set that differs from modality to modality. We generate these sets with the ABC algorithm developed by Karaboğa et al. The algorithm needs different coefficient sets for different tasks; for example, the coefficient set generated for the T1 modality images is not suitable for the PD or T2 modality images. The coefficient set generated for the T1 images is also applied to the T1-FLASH and T1-MP-RAGE images. In our work, we also generate sets for segmenting different regions in brain images, where proper coefficient sets in the WM region, CC region, or the entire brain can be segmented or emphasized in the image.

In case study 1, the algorithm performs best with the T1 modality images with 5.844 CIR, 6.217 EME, 15.045 AMBE, and 22.150 dB PSNR scores as average values. The algorithm also performs adequately well with the T2 and PD images. Evaluation scores of the T2 images processed with the CEULICA are 4.736 CIR, 9.251 EME, 17.652 AMBE, and 12.680 dB PSNR scores as average values. Evaluation scores of the PD images processed with the CEULICA are 3.594 CIR, 4.871 EME, 6.209 AMBE, and 17.211 dB PSNR. However, the T2 and PD scores still need to be improved with extra research on linear combination coefficients.

In case study 2, the algorithm performs best with the T1-MP-RAGE modality images with 6.983 CIR, 17.326 EME, 3.514 AMBE, and 30.157 dB PSNR scores as average values. The algorithm's performance with the T1-FLASH modality images gives satisfactory results with 10.191 CIR, 12.820 EME, 2.884 AMBE, and 30.948 dB PSNR scores as average values. Evaluation scores of the T2-type images in the MIDAS database processed with the CEULICA are scored as 2.705 CIR, 73.111 EME, 12.683 AMBE, and 20.240 dB PSNR as average values.

The CEULICA can be used for classification tasks with proper linear combination coefficients, for instance, classification of the WM regions in brain MRI images. For this purpose, the only need is to find the right coefficient sets for classifications. Thus, 3 coefficient sets are generated: the T1, T2, and PD modality images. In this study, a brief representation of this classification ability of the algorithm is done.

In future studies, we aim to generate effective coefficient sets for all image types. Moreover, we aim to develop an adaptive version of the algorithm for automatically detecting and adapting itself for any given image. Another aim is also developing a segmentation algorithm based on or supported by the CEULICA.

Acknowledgments

The MR brain images from healthy volunteers used in this paper were collected and made available by the CASILab at The University of North Carolina at Chapel Hill and were distributed by the MIDAS Data Server at Kitware, Inc.

References

[1] K. Nakamura, E. Fisher, "Segmentation of brain magnetic resonance images for measurement of gray matter atrophy in multiple sclerosis patients", Neuroimage, Vol. 44, pp. 769–776, 2009.

[2] J. Hwang, J. Kim, Y. Han, H. Park, "An automatic cerebellum extraction method in T1-weighted brain MR images using an active contour model with a shape prior", Magnetic Resonance Imaging, Vol. 29, pp. 1014–1022, 2011.

[3] K. Van Leemput, F. Maes, D. Vandermeulen, A. Colchester, P. Suetens, "Automated segmentation of multiple sclerosis lesions by model outlier detection", IEEE Transactions on Medical Imaging, Vol. 20, pp. 677–688, 2001.

[4] J. Xue, A. Pizurica, W. Philips, E. Kerre, R. Van De Walle, I. Lemahieu, "An integrated method of adaptive enhancement for unsupervised segmentation of MRI brain images", Pattern Recognition Letters, Vol. 24, pp. 2549–2560, 2003.

[5] A. Khademi, A. Venetsanopoulos, A. Moody, "Automatic contrast enhancement of white matter lesions in FLAIR MRI", IEEE International Symposium on Biomedical Imaging: From Nano to Macro, pp. 322–325, 2009.

[6] A. Majumder, S. Irani, "Contrast enhancement of images using human contrast sensitivity", Proceedings of the 3rd Symposium on Applied Perception in Graphics and Visualization, pp. 69–76, 2006.

[7] M.H. Kabir, M. Abdullah-Al-Wadud, O. Chae, "Brightness preserving image contrast enhancement using weighted mixture of global and local transformation functions", Proceedings of the International Arab Journal of Information Technology, Vol. 7, pp. 403–410, 2010.

[8] O. Kosheleva, J. Arenas, M. Aguirre, C. Mendoza, S.D. Cabrera, "Compression degradation metrics for analysis of consistency in microcalcification detection", IEEE Southwest Symposium on Image Analysis and Interpretation, pp. 35–40, 1998.

[9] K.A. Panetta, E.J. Wharton, S.S. Agaian, "Human visual system-based image enhancement and logarithmic contrast measure", IEEE Transactions on Systems, Man, and Cybernetics, Part B: Cybernetics, Vol. 38, pp. 174–188, 2008.

[10] Z.Y. Chen, B.R. Abidi, L. David, M.A. Abidi, "Gray-level grouping (GLG): an automatic method for optimized image contrast enhancement - part II: the variations", IEEE Transactions on Image Processing, Vol. 15, pp. 2303–2314, 2006.

[11] R.L. Smathers, E. Bush, J. Drace, M. Stevens, F.G. Sommer, B.W. Brown, B. Kanas, "Mammographic microcalcifications: Detection with xerography, screen-film and digitized film display", Radiology, Vol. 159, pp. 673–677, 1986.

[12] H.Y. Yang, Y.C. Lee, Y.C. Fan, H.W. Taso, "A novel algorithm of local contrast enhancement for medical image", IEEE Nuclear Science Symposium Conference Record, Vol. 5 pp. 3951–3954, 2007.

[13] M. Vidaurrazaga, L.A. Diago, A. Cruz, "Contrast enhancement with wavelet transform in radiological images", Proceedings of the 22nd Annual International Conference of the IEEE Engineering in Medicine and Biology Society, Vol. 3, pp. 1760–1763, 2000.

[14] D. Karaboga, B. Gorkemli, C. Ozturk, N. Karaboga, "A comprehensive survey: artificial bee colony (ABC) algorithm and applications", Artificial Intelligence Review, pp. 1–37, 2012.

[15] D. Karaboga, B. Akay, "A survey: algorithms simulating bee swarm intelligence", Artificial Intelligence Review, Vol. 31, pp. 61–85, 2009.

[16] S. Grgić, M. Grgić, M. Mrak, "Reliability of objective picture quality measures", Journal of Electrical Engineering, Vol. 55, pp. 3–10, 2004.

[17] M. Sundaram, K. Ramar, N. Arumugam, G. Prabin, "Histogram modified local contrast enhancement for mammogram images", Applied Soft Computing, Vol. 11, pp. 5809–5816, 2011.

[18] Z. Wang, A.C. Bovik, "A universal image quality index", IEEE Signal Processing Letters, Vol. 9, pp. 81–84, 2002.

[19] BrainWeb: Simulated Brain Database, http://www.bic.mni.mcgill.ca/brainweb/, Last accessed: 03 June 2012.

[20] C.A. Cocosco, V. Kollokian, R.K.S. Kwan, A.C. Evans, "BrainWeb: Online interface to a 3D MRI simulated brain database", NeuroImage, Vol. 5, S 425, 1997.

[21] R.K.S. Kwan, A.C. Evans, G.B. Pike, "MRI simulation-based evaluation of image-processing and classification methods", IEEE Transactions on Medical Imaging, Vol. 18, pp. 1085–1097, 1999.

[22] R.K.S. Kwan, A.C. Evans, G.B. Pike, "An extensible MRI simulator for post-processing evaluation", Lecture Notes in Computer Science, Vol. 1131, pp. 135–140, 1996.

[23] D.L. Collins, A.P. Zijdenbos, V. Kollokian, J.G. Sled, N.J. Kabani, C.J. Holmes, A.C. Evans, "Design and construction of a realistic digital brain phantom", IEEE Transactions on Medical Imaging, Vol. 17, pp. 463–468, 1998.

[24] E. Bullitt, D. Zeng, G. Gerig, S. Aylward, S. Joshi, J.K. Smith, W. Lin, M.G. Ewend, "Vessel tortuosity and brain tumor malignancy: a blinded study", Academic Radiology, Vol. 12, pp. 1232–1240, 2005.